BİTLİS EREN ÜNİVERSİTESİ
FEN BİLİMLERİ DERGİSİ

ISSN: 2147-3129 / e-ISSN: 2147-3188

Article Type	: Research Article	**Year**	: 2025
Received	: December 16, 2024	**Volume**	: 14
Revised	: January 17, 2025	**Issue**	: 1
Accepted	: January 24, 2025	**Pages**	: 494-512
DOI	: 10.17798/bitlisfen.1602308		

IDENTIFIABILITY ANALYSIS OF A MATHEMATICAL MODEL FOR THE FIRST WAVE OF COVID-19 IN TÜRKİYE

Tuğba AKMAN [1]

[1] *University of Turkish Aeronautical Association, Department of Computer Engineering, Ankara, Türkiye,* takman@thk.edu.tr

ABSTRACT

In this work, a structurally identifiable mathematical model is developed to capture the first peak of COVID-19 in Türkiye. The daily numbers of COVID-19 cases, deaths, prevalence in the ICU, and prevalence on ventilation, obtained from the open-access TURCOVID-19 database, during the first peak, are used as observations. Structural identifiability analysis is performed using the open-source software Julia. For parameter estimation, some parameters are fixed based on the literature while the remaining parameters are estimated using the Data2Dynamics software. Our results align well with the observations. Then, a practical identifiability analysis based on the profile likelihood method is conducted to investigate uncertainties in the parameter values. It reveals that three of the model parameters, namely the progression rate of symptomatically infectious individuals to hospital and the transmission rates associated with exposed and symptomatically infectious individuals, are not practically identifiable. This means that the implementation of intervention strategies via this model must be performed carefully.

Keywords: Structural identifiability, Practical identifiability, COVID-19, Mathematical modeling, Türkiye.

1 INTRODUCTION

The novel coronavirus has changed the world in several ways, such as introducing new hygiene habits, emphasizing effective handwashing, skipping the handshake, working out at home, increasing reliance on online meetings, and raising awareness about vaccination or boosters. Once a novel virus began affecting the world, predicting the number of infectious

individuals, forecasting upcoming peaks, and determining the most suitable public interventions became crucial.

Researchers and scientists have paid attention to mathematical models in infectious disease modeling for decision-making. Intervention strategies and their impacts are compared using run charts, EWMA control charts, and p-control charts based on COVID-19 data from Türkiye [1]. An algorithm approximating the effect of nodes in complex networks has been developed under the susceptible-infectious-recovered (SIR) models [2]. We refer the reader to the studies for reviews on COVID-19 modeling (see, examples [3-5].). On the other hand, hypothetical models have gained importance in understanding the spread of the disease within communities. In particular, the potential use of face masks has been investigated in mathematical models; the importance of face masks together with non-pharmaceutical interventions is concluded [6]. As more data have been collected, models incorporating parameter estimation methods have revealed country-based differences driven by intervention strategies, human behavior, and technology. For example, differences have been observed in India, Mexico, Wuhan, Sweden, Canada, and Türkiye [7-12]. Vaccination programs have been examined through mathematical models, with findings suggesting that vaccination alone is not sufficient to control the spread [13]. The effects of awareness programs have also been studied, with results indicating that awareness and timely hospitalization are critical factors in eliminating the disease [14]. The impact of testing and isolation has been discussed, and authors have concluded that the timing of testing and the rate of testing are two key factors in developing effective control strategies [15]. Malik et al. have expressed the outbreak of COVID-19 as a fractional order system and considered an inverse problem to find the time-dependent parameters in the model for the data of India [16, 17].

The construction of a mathematical model consists of several steps [18, Figure. 1]. Model development is followed by structural identifiability analysis. This is necessary because two different parameter sets can sometimes lead to the same solution curves for a structurally nonidentifiable model. However, this can result in unrealistic model behavior. In fact, inefficient control strategies based on such models may cause the disease to spread even more. Therefore, it is crucial to analyze whether the model is structurally identifiable before proceeding with model calibration. Model calibration enables the determination of the parameter values in the model. While model parameters are structurally identifiable, they may not always be practically identifiable. Therefore, practical identifiability analysis is essential. If any parameter is found

to be practically nonidentifiable, then one must be careful in making predictions or adjustments in case of parameter perturbations.

Akman et al. constructed a mathematical model for COVID-19 in Türkiye [12], which captured the first peak using the data from the TURCOVID-19 database [19]. They also investigated the effect of underreporting [12]. In this work, we extend the model presented in the work [12] by splitting the symptomatically infectious subgroup into symptomatically infectious and hospitalized patients and adding a quarantine subgroup to model the first peak of the spread. Additionally, we investigate both the structural and practical identifiability of the model, which were not within the scope of the paper by Akman et al. [12]. From this current study, we have learned that caution is needed when making future predictions or planning interventions based on this model, as α_1, β_e, and β_s (the progression rate of symptomatically infectious individuals to hospital, and the transmission rates associated with exposed and symptomatically infectious individuals) are not practically identifiable. The rest of the paper is organized as follows: In Sec. 2, the mathematical model is developed and explained. Sec. 3 presents the structural identifiability analysis. Sec. 4 is devoted to model calibration, followed by the practical identifiability analysis in Sec. 5. Sensitivity analysis is discussed in Sec. 6. Simulation results are presented in Sec.7. This paper ends with a summary and conclusion.

2 MODEL DEVELOPMENT

We develop a mathematical model for the first wave of COVID-19 by splitting the total population of Türkiye at time t, denoted N(t), into nine mutually exclusive compartments of individuals for the period of March 11, 2020 - May 31, 2020. The variables in the model represent the number of individuals in each compartment: susceptible S:=S(t), exposed E:=E(t), asymptomatic and infectious but not tested I_n:=I_n(t), symptomatic and infectious I_s:=I_s(t), hospitalized and isolated I_h:=I_h(t), patients staying at ICU I_{ICU}:=I_{ICU}(t), ventilated I_v:=I_v(t), recovered R:=R(t) and quarantined Q:=Q(t) at time t. Therefore, the total population N:=N(t) is given by

$$N = S + E + I_n + I_s + I_h + I_{ICU} + I_v + R + Q.$$

We use the standard incidence and exclude isolated individuals, as motivated by the work [21], in the disease transmission state. Susceptible individuals (S) become infected because of the interactions with exposed individuals (E), asymptomatically infectious individuals (I_n), and symptomatically infectious individuals (I_s) at the rates of β_e, β_n, and β_s,

respectively. The exposed class (E) is affected by this interaction, and the exposed compartment decreases at the rate of k. A fraction ρ of exposed individuals show symptoms, while the rest move to the compartment of asymptomatically infectious individuals (I_n). Asymptomatically and symptomatically infectious individuals recover at the rates of γ_n and γ_s, respectively. Symptomatically infectious individuals may develop severe infections and get hospitalized at the rate of α_1. Hospitalized individuals die at the rate of μ_h and recover at the rate of γ_h. Hospitalized patients may be transferred to the ICU at the rate of α_2, and ICU patients may be ventilated (I_v) at the rate of α_3. Both ICU patients and ventilated patients recover at the rates of γ_{ICU} and γ_v, respectively, and pass away at the rates of μ_{ICU} and μ_v, respectively. During simulations, quarantine and isolation strategies are implemented, so susceptible individuals move to quarantine at the rate of c. We exclude quarantine of the subgroups of E, I_n and I_s, as quarantine is applied only when the number of infectious individuals becomes too high. Since we are modeling the early stages of the pandemic, we exclude the terms for natural death, births, and vaccination. Based on these assumptions, we develop the following model:

$$\frac{dS}{dt} = -(\beta_e E + \beta_n I_n + \beta_s I_s)\frac{S}{N - I_h - I_{ICU} - I_v - Q} - \eta S, \tag{1a}$$

$$\frac{\mathrm{dE}}{dt} = (\beta_e E + \beta_n I_n + \beta_s I_s)\frac{S}{N - I_h - I_{ICU} - I_v - Q} - kE, \tag{1b}$$

$$\frac{\mathrm{d}I_n}{dt} = (1-\rho)kE - \gamma_n I_n, \tag{1c}$$

$$\frac{\mathrm{d}I_s}{dt} = \rho kE - (\alpha_1 + \gamma_s) I_s, \tag{1d}$$

$$\frac{\mathrm{d}I_h}{dt} = \alpha_1 I_s - (\alpha_2 + \gamma_h + \mu_h) I_h, \tag{1e}$$

$$\frac{\mathrm{d}I_{ICU}}{dt} = \alpha_2 I_h - (\alpha_3 + \gamma_{ICU} + \mu_{ICU}) I_{ICU}, \tag{1f}$$

$$\frac{\mathrm{d}I_v}{dt} = \alpha_3 I_{ICU} - (\gamma_v + \mu_v) I_v, \tag{1g}$$

$$\frac{\mathrm{dR}}{dt} = \gamma_n I_n + \gamma_s I_s + \gamma_h I_h + \gamma_{ICU} I_{ICU} + \gamma_v I_{v,} \tag{1h}$$

$$\frac{\mathrm{dQ}}{dt} = \eta S, \tag{1i}$$

$$S(0) = S_0, E(0) = E_0, I_n(0) = I_{n,0}, I_s(0) = I_{s,0}, I_h(0) = I_{h,0}, I_{ICU}(0) = I_{ICU,0}, I_v(0) = I_{v,0}\ R(0) = R_{n,0}, \mathrm{Q}(0) = Q_{n,0}. \tag{1j}$$

We proceed with the proofs of existence and uniqueness, positivity and boundedness of the solution.

2.1 Model analysis

We observe that the right-hand side of model (1) is completely continuous and locally Lipschitzian. Therefore, its solution, namely S(t), E(t), $I_n(t)$, $I_s(t)$, $I_h(t)$, $I_{icu}(t)$, $I_v(t)$, R(t), and Q(t), with non-negative initial conditions exists and is unique on the interval [0, t*], where $0 < t^* < \infty$ [22].

We first prove that the solution is positive. Consider $t^* = \sup\{t > 0: S(t), E(t), I_n(t), I_s(t), I_h(t), I_{icu}(t), I_v(t), R(t), Q(t) > 0\}$. Then, by integration, Equation (1a) leads to

$$\frac{d}{dt}(S(t)\, exp(\eta t + \int_0^{t*} \frac{\beta_e E(u) + \beta_n I_n(u) + \beta_s I_s(u)}{N(u) - I_h(u) - I_{ICU}(u) - I_v(u) - Q(u)}\, du)) = 0.$$

Then, we obtain

$$S(t*)\, exp(\eta t* + \int_0^{t*} \frac{\beta_e E(u) + \beta_n I_n(u) + \beta_s I_s(u)}{N(u) - I_h(u) - I_{ICU}(u) - I_v(u) - Q(u)}\, du) - S(0) = 0.$$

We rewrite this equation to reach

$$S(t*) = S(0)\, exp(-\eta t* - \int_0^{t*} \frac{\beta_e E(u) + \beta_n I_n(u) + \beta_s I_s(u)}{N(u) - I_h(u) - I_{ICU}(u) - I_v(u) - Q(u)}\, du) \geq 0.$$

It means that the solution S(t) is non-negative. Similarly, we can follow the same approach to prove that all other solutions are non-negative.

We secondly prove that the model variables are bounded above. Therefore, we add all the equations up in model (1) to obtain

$$\frac{dN}{dt} = -\mu_h I_h - \mu_{icu} I_{icu} - \mu_v I_v \leq -min(\mu_h, \mu_{icu}, \mu_v)\, N = -\mu\, N,$$

where $min(\mu_h, \mu_{icu}, \mu_v) = \mu$. We observe that N is a decreasing function of time t and $N(t) = N(0)exp(-\mu\, t)$. Then, it means that all model variables are bounded above. We now proceed with the structural identifiability analysis.

3 STRUCTURAL IDENTIFIABILITY ANALYSIS

Identifiability analysis has been discussed in many studies (for example [23-27]). Here, we provide a summary based on these works.

A model parameter p_i is called identifiable if the confidence interval associated with p_i, denoted $[p^+_i , p^-_i]$, is finite. There are two types of identifiability that can be investigated: structural and practical identifiability. The former is independent of the data and concerns the

structure of the mathematical model, while the latter considers the observations used for model fitting. Some mathematical models suffer from structural nonidentifiability, meaning that a unique parametrization of the model using the available observations cannot be achieved.

We, firstly, investigate the structural identifiability of model (1) by expressing it as

$$x'(t) = f(x,p), \qquad x(0) = x0, \tag{2}$$

where x and p denote the states and parameters of model (1), respectively. The data in this study comes from the open-access TURCOVID-19 database [28, 19]. The observations we have are the daily number of cases $y_1(t) = \rho kE$, the daily number of deaths $y_2(t) = \mu_h I_h + \mu_{ICU} I_{ICU} + \mu_v I_v$, ICU prevalence $y_3(t) = I_{ICU}$ and ventilation unit prevalence $y_4(t) = I_v$. We can write the observations as:

$$y(t) = g(x,p) \ . \tag{3}$$

The model given by Equation (2) is structurally identifiable if the vector p can be uniquely determined from the observations y(t) in Equation (3), assuming the observations are unlimited [23]. Otherwise, the model is considered unidentifiable. The formal definition is provided below [29].

Definition 1. Suppose that p and p̲ are two distinct parameter vectors. Model (1) is said to be globally (uniquely) structurally identifiable if

$$g(x,p) = g(x,\underline{p}) \quad implies \quad p = \underline{p}. \tag{4}$$

Definition 2. Model (1) is said to be locally structurally identifiable if for any p within an open neighborhood of p̲ in the parameter space,

$$g(x,p) = g(x,\underline{p}) \quad implies \quad p = \underline{p}. \tag{5}$$

Structural identifiability can be analyzed using various methods, such as the Taylor series method [30], Lie symmetries [31], generating power series approach [32], and differential algebra approach [33]. We prefer the differential algebra approach as the open-source software JULIA [33] and its structural identifiability package [25, 35] can perform this analysis and can capture both identifiable and nonidentifiable parameters. The differential algebra approach explains the structural identifiability as follows [36]:

Definition 3. Suppose that c(**p**) denotes the coefficients of the input-output equation corresponding to model (1). We say that model (1) is structurally identifiable from unlimited observations y(t) if and only if c(**p**) = c(**p̲**) implies **p** = **p̲**.

If a model is not structurally identifiable, reparametrization is required [37].

4 MODEL CALIBRATION

We proceed with parameter estimation for model (1) using the data obtained from the online database TURCOVID19 [19, 28]. The spread of the virus in the community changes over time due to public interventions. Therefore, we focus on the early dynamics of the spread, during which we can capture the first peak, specifically the period from March 11, 2020, to May 31, 2020, in Türkiye. We fit model (1) to the data, including the number of COVID-19 cases, the number of deaths, ICU prevalence, and ventilation prevalence. Let $\{t_i\}_{i=1}^{k_1}, \{t_i\}_{i=1}^{k_2}, \{t_i\}_{i=1}^{k_3}$ and $\{t_i\}_{i=1}^{k_4}$ represent the time points for each observation, respectively. The measurements contain some noise and can be expressed as

$$
\begin{aligned}
Y_1^i &= y_1(t_i) + \epsilon_i, \quad i = 1,2,\cdots,k_1,\\
Y_2^i &= y_2(t_i) + \epsilon_i, \quad i = 1,2,\cdots,k_2,\\
Y_3^i &= y_3(t_i) + \epsilon_i, \quad i = 1,2,\cdots,k_3,\\
Y_4^i &= y_4(t_i) + \epsilon_i, \quad i = 1,2,\cdots,k_4.
\end{aligned} \tag{6}
$$

We estimate the parameters of model (1) by solving the following optimization problem:

$$
\min\ p\left(\frac{1}{k_1}\sum_{i=1}^{k_1}\frac{|y_1(t_i)-Y_1^i|^2}{\tilde{Y}_1^2} + \frac{1}{k_2}\sum_{i=1}^{k_2}\frac{|y_2(t_i)-Y_2^i|^2}{\tilde{Y}_2^2} + \frac{1}{k_3}\sum_{i=1}^{k_3}\frac{|y_3(t_i)-Y_3^i|^2}{\tilde{Y}_3^2} + \right.
$$

$$
\left. + \frac{1}{k_4}\sum_{i=1}^{k_4}\frac{|y_4(t_i)-Y_4^i|^2}{\tilde{Y}_4^2}\right), \tag{7}
$$

$$
\text{w. r. t. the constraint } p > 0. \tag{8}
$$

The terms $\tilde{Y}_t^i$ for $t \in \{1, 2, 3, 4\}$ are the average observations written as $\tilde{Y}_t^i = \frac{1}{k_t}\sum_{i=1}^{k_t} Y_t$.

After model calibration, practical identifiability is performed to investigate the confidence intervals of the model parameters.

5 PRACTICAL IDENTIFIABILITY ANALYSIS

We proceed with the practical identifiability analysis, as model (1) has been shown to be structurally identifiable. However, a structurally identifiable parameter may still be practically nonidentifiable. This often occurs when the observations or data used in model calibration are insufficient to compute a finite confidence interval [38]. It is defined as follows:

Definition 4. A parameter estimate p_i is practically nonidentifiable; despite the unique minimum of the likelihood for this parameter, the likelihood-based confidence region associated with the parameter is infinitely extended in increasing and/or decreasing direction of p_i.

There are several methods to analyze parameter identifiability, including Bayesian sampling approaches [39, 40], bootstrap methods [41], and the Fisher information matrix [42]. Additionally, using the profile likelihood method [23, 24], we can determine the practically identifiable parameters with a 95% confidence interval, allowing us to assess parameter uncertainties in the model. We prefer this approach because it can be easily implemented using the d2d software after model calibration [43-45].

6 SENSITIVITY ANALYSIS

Global sensitivity analysis is performed for COVID-19 models to test the robustness of the model [12, 46]. In this work, the method of the partial rank correlation coefficient (PRCC) is used [47]. The aim is to measure the effect of each model parameter on a variable or observation to obtain a value between −1 and +1 and to determine the strength of this value. Computational details and simulation results are discussed in the next section.

7 SIMULATION RESULTS

After constructing the model and determining the type of data to use, we perform structural identifiability analysis. We use the open-source software JULIA [34] and its StructuralIdentifiability.jl package [25, 35] for the analysis.

However, we encountered a memory error in JULIA. This issue can be resolved by using linear first integrals, which speed up computations [46]. We apply a suitable transformation to the model (1) to eliminate one of the unknowns in the system. Details are provided in the appendix.

Based on the analysis performed in JULIA [33], we find that all variables and parameters of model (1) are globally identifiable. After confirming that the model is structurally identifiable, we proceed with parameter estimation using the d2d software [43-45]. We fix the values of some parameters related to the dynamics of COVID-19 based on the literature. The d2d software uses a deterministic optimisation algorithm, namely lsqnonlin, in the parameter estimation step [44]. In addition, the d2d software decides the most efficient ODE solver to find the numerical solution. The parameter interval is set as $p \in (10^{-6}, 10^{5})$, with the upper bound for α_1 is fixed as 10^{11} and the lower bounds for β_e and β_s are set as 10^{-8}. The values of parameters and initial conditions are provided in Table 1.

Table 1. Parameter values.

Parameter	Value	Unit	Source
α_1	2.8×10^{10}	Day^{-1}	Calibrated
α_2	0.041	Day^{-1}	Calibrated
α_3	0.14	Day^{-1}	Calibrated
β_e	1.4×10^{-9}	Day^{-1}	Calibrated
β_n	1.7	Day^{-1}	Calibrated
β_s	6.3×10^{-6}	Day^{-1}	Calibrated
η	0.19	Day^{-1}	Calibrated
γ_h	0.1449	Day^{-1}	[47]
γ_{ICU}	0.231285	Day^{-1}	[47]
γ_n	0.3448	Day^{-1}	[47]
γ_s	0.1429	Day^{-1}	[47]
γ_v	0.239209	Day^{-1}	[47]
k	1/14	Day^{-1}	Estimated from [48]
μ_{ICU}	0.0605032	Day^{-1}	[12]
μ_h	0.000001	Day^{-1}	Adapted from [12]
μ_v	0.00029338	Day^{-1}	[12]
ρ	0.28	Day^{-1}	[12]
S_0	8×10^{7}	Individual	[12]
E_0	437	Individual	[12]
$I_{n,0}$	490	Individual	[12]
$I_{s,0}$	1	Individual	Data
$I_{h,0}$, $I_{ICU,0}$, $I_{hv,0}$, $R_{h,0}$, $Q_{h,0}$	0	Individual	Data

The optimization problem (7)-(8) is solved as a multi-start optimization problem with 500 iterations. Figure 1 shows that convergence is achieved, and the first-order optimality criterion is calculated as 3.82169×10^{-8}.

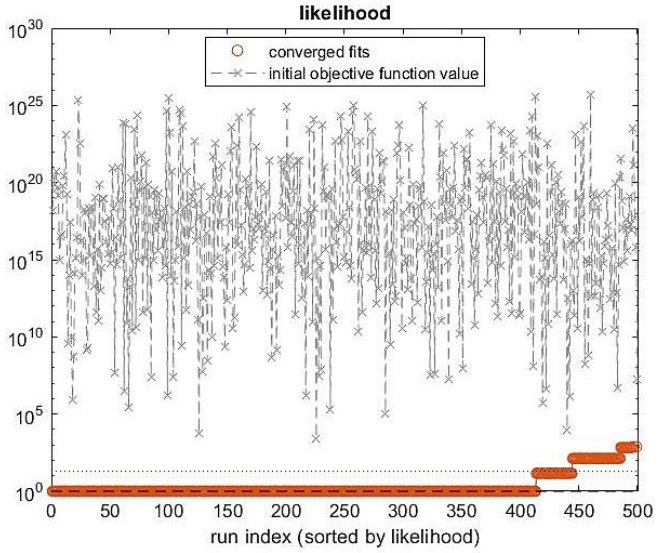

Figure 1. Overview about the multistart optimization.

We present the simulation results in Figure. 2-5. We observe that model (1) accurately predicts the dynamics, and the simulation results align well with the model observations.

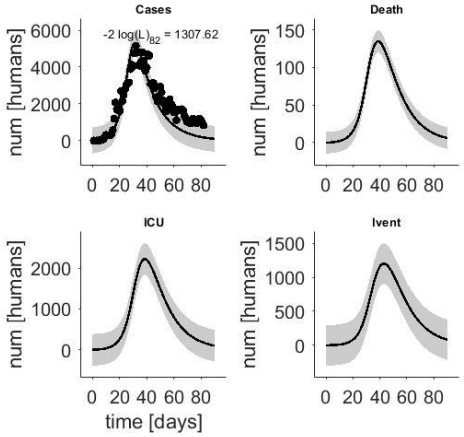

Figure 2. Simulation results for the number of cases.

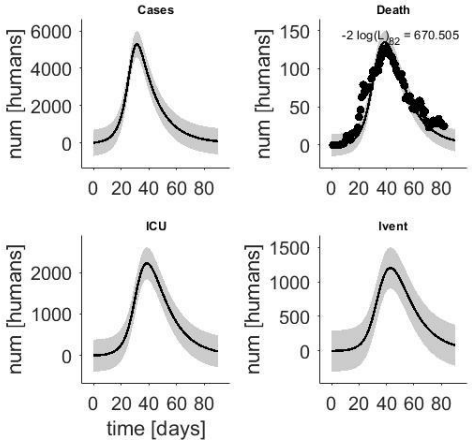

Figure 3. Simulation results for the number of deaths.

After model calibration, we proceed with the practical identifiability analysis using profile likelihood, which is performed by the d2d software.

We note that calibrated parameter values p_i's are displayed by gray stars, and thresholds for the confidence intervals are shown by the upper and lower dashed lines in Figure 6. We note that calibrated parameter values p_i's are displayed by gray stars, and thresholds for the confidence intervals are shown by the upper and lower dashed lines in Figure 4. We observe that the parameters α_1, β_e, and β_s are not practically identifiable, as a finite confidence interval for α_1 and β_e cannot be determined, and the confidence interval for β_s is very flat. The value of β_e is found at the left end of the parameter interval, indicating practical nonidentifiability. To overcome this, additional data sets should be incorporated during the model calibration step, such as data on the number of susceptible individuals. However, such data are difficult to collect, as it is not possible to test everyone in the population to determine whether they are infectious.

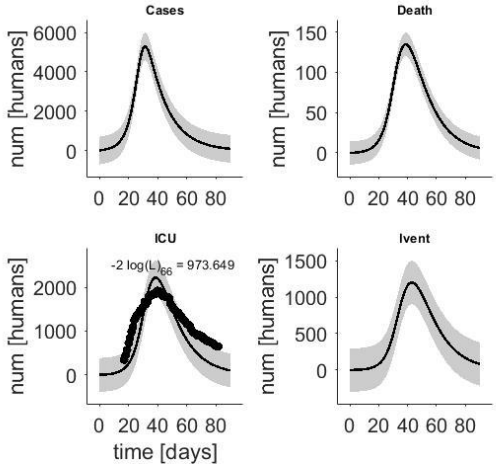

Figure 4. Simulation results for ICU prevalence.

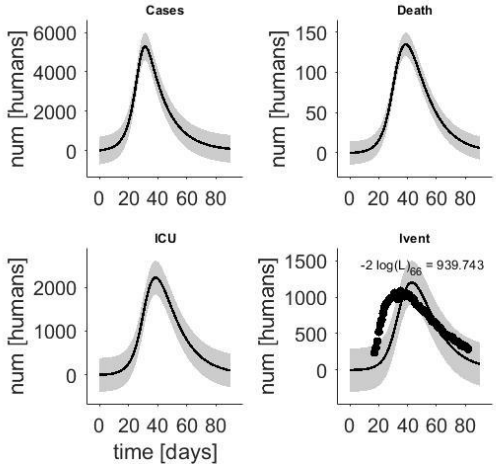

Figure 5. Simulation results for ventilation prevalence.

We proceed with sensitivity analysis. A MATLAB code developed by Lab has been modified for implementation of the method of PRCC [48]. Intervals for each parameter are set starting from half to twice the baseline value, and a uniformly distributed sample space with 1000 sample values is constructed.

We investigate the sensitivities of the number of cases and the number of deaths and present them in Figure. 7 and Figure. 8, respectively. We choose the days corresponding to the middle and the end of the simulation interval, namely days 40 and 80, respectively, for comparison purposes. We observe that the number of cases increases as the parameter β_n increases, while it decreases as the rate of quarantine, the rate of recovery for asymptomatically infectious.

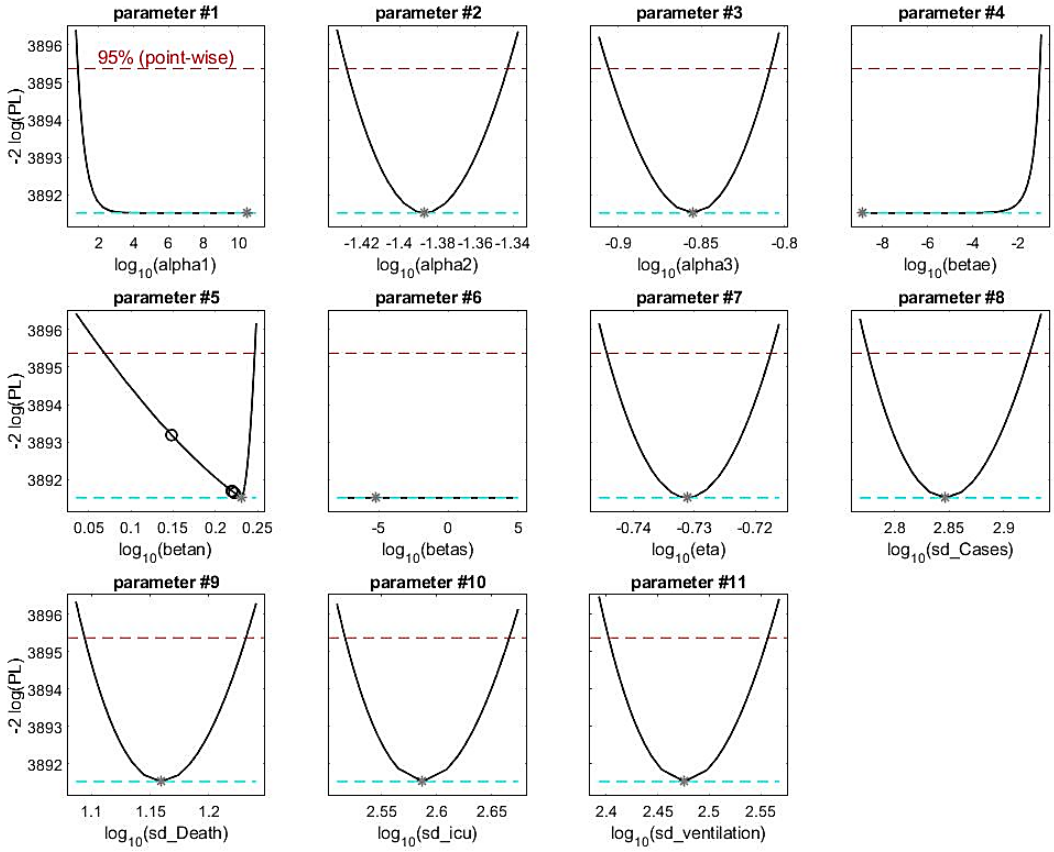

Figure 6. Profile likelihood curves.

For day 80, it is inversely proportional to the incubation period 1/k. On the other hand, the number of deaths is proportional to the parameters β_n and α_2. It means that as the value of the transmission rate and the rate at which patients are transferred to ICU increases, the more people pass away. Negative, but the largest sensitivity in magnitude occurs for the parameter η meaning that as the rate of quarantine increases, more lives can be saved.

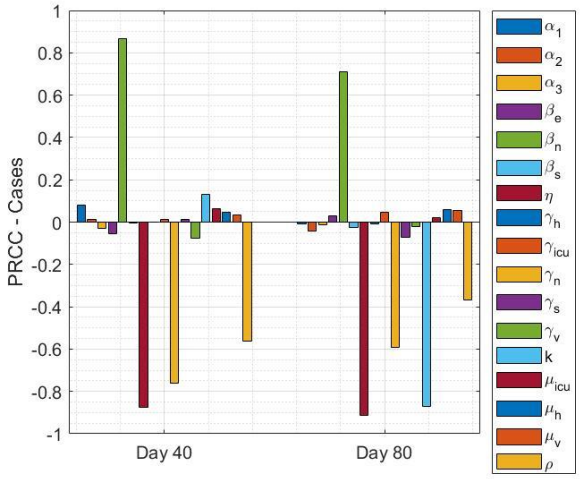

Figure 7. Sensitivity analysis for the number of cases.

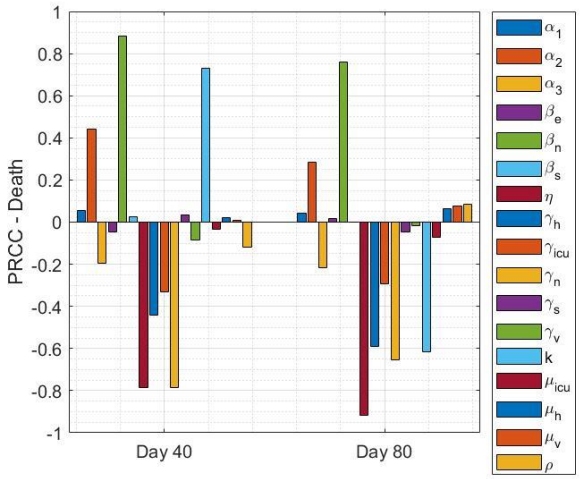

Figure 8. Sensitivity analysis for the number of deaths.

8 CONCLUSION AND SUGGESTIONS

We develop a model for disease transmission during the first peak of COVID-19 in Türkiye. We observe that our model is structurally identifiable when using the number of symptomatic cases, deaths, patients in the ICU, and ventilated patients as observations. Structural identifiability analysis is performed using the open-source software Julia and its structural identifiability package after simplifying the model based on linear first integrals. Model calibration is carried out as a multi-start optimization problem, and the simulation results align well with the data. Next, we investigate the variability of the parameters based on the profile likelihood method for parameter identifiability. We find that the parameters α_1, β_e, and β_s are not practically identifiable. It indicates that the implementation of intervention strategies

must be carried out with caution. In addition, we performed sensitivity analysis and determined the effect of the parameters on the observations, namely the number of cases and deaths. The disease transmission rate of asymptomatically infectious individuals and the rate of quarantine have the biggest impact on the observations. Indeed, the former is positively correlated, the latter is negatively correlated with the observations.

As future work, this model can be extended to model subsequent waves of the pandemic by incorporating delay terms, and the identifiability of the models developed for vaccination strategies can be investigated.

Acknowledgment

The author would like to thank the anonymous reviewers for the constructive feedback.

Statement of Research and Publication Ethics

The study is compiled with research and publication ethics.

Artificial Intelligence (AI) Contribution Statement

This manuscript was entirely written, edited, analyzed, and prepared without the assistance of any artificial intelligence (AI) tools. All content, including text, data analysis, and figures, was solely generated by the authors.

REFERENCES

[1] E. Polat, "Using quality control charts for monitoring COVID-19 daily cases and deaths in Türkiye," *Bitlis Eren Üniversitesi Fen Bilimleri Dergisi*, vol. 13, no. 1, pp. 134–152.

[2] A. Şimşek, "Estimating the expected influence capacities of nodes in complex networks under the susceptible-infectious-recovered model," *Bitlis Eren Üniversitesi Fen Bilimleri Dergisi*, vol. 13, no. 2, pp. 408–417.

[3] R. Padmanabhan, H. S. Abed, N. Meskin, T. Khattab, M. Shraim, and M. A. Al-Hitmi, "A review of mathematical model-based scenario analysis and interventions for COVID-19," *Computer Methods and Programs in Biomedicine*, vol. 209, p. 106301, 2021.

[4] I. Rahimi, F. Chen, and A. H. Gandomi, "A review on COVID-19 forecasting models," *Neural Computing and Applications*, vol. 35, no. 33, pp. 23671–23681, 2023.

[5] Y. Xiang, Y. Jia, L. Chen, L. Guo, B. Shu, and E. Long, "COVID-19 epidemic prediction and the impact of public health interventions: A review of COVID-19 epidemic models," *Infectious Disease Modelling*, vol. 6, pp. 324–342, 2021.

[6] S. E. Eikenberry, M. Mancuso, E. Iboi, T. Phan, K. Eikenberry, Y. Kuang, E. Kostelich, and A. B. Gumel, "To mask or not to mask: Modeling the potential for face mask use by the general public to curtail the COVID-19 pandemic," *Infectious Disease Modelling*, vol. 5, pp. 293–308, 2020.

[7] S. K. Biswas, J. K. Ghosh, S. Sarkar, and U. Ghosh, "COVID-19 pandemic in India: a mathematical model study," *Nonlinear Dynamics*, vol. 102, pp. 537–553, 2020.

[8] O. Torrealba-Rodriguez, R. Conde-Gutiérrez, and A. Hernández-Javier, "Modeling and prediction of COVID-19 in Mexico applying mathematical and computational models," *Chaos, Solitons & Fractals*, vol. 138, p. 109946, 2020.

[9] A. J. Kucharski, T. W. Russell, C. Diamond, Y. Liu, J. Edmunds, S. Funk, R. M. Eggo, F. Sun, M. Jit, and J. D. Munday, "Early dynamics of transmission and control of COVID-19: a mathematical modelling study," *The Lancet Infectious Diseases*, vol. 20, no. 5, pp. 553–558, 2020.

[10] M. Carlsson and C. Söderberg-Nauclér, "COVID-19 modeling outcome versus reality in Sweden," *Viruses*, vol. 14, no. 8, p. 1840, 2022.

[11] A. R. Tuite, D. N. Fisman, and A. L. Greer, "Mathematical modelling of COVID-19 transmission and mitigation strategies in the population of Ontario, Canada," *CMAJ*, vol. 192, no. 19, pp. E497–E505, 2020.

[12] T. Akman, E. Köse, and N. Tuncer, "Assessment of vaccination and underreporting on COVID-19 infections in based on effective reproduction number," *International Journal of Biomathematics*, pp. 2350102 – Online ready, 2024. [Online]. Available: https://doi.org/10.1142/S1793524523501024

[13] S. Moore, E. M. Hill, M. J. Tildesley, L. Dyson, and M. J. Keeling, "Vaccination and non-pharmaceutical interventions for COVID-19: a mathematical modelling study," *The Lancet Infectious Diseases*, vol. 21, no. 6, pp. 793–802, 2021.

[14] S. S. Musa, S. Qureshi, S. Zhao, A. Yusuf, U. T. Mustapha, and D. He, "Mathematical modeling of COVID-19 epidemic with effect of awareness programs," *Infectious Disease Modelling*, vol. 6, pp. 448–460, 2021.

[15] S. Gao, P. Binod, C. W. Chukwu, T. Kwofie, S. Safdar, L. Newman, S. Choe, B. K. Datta, W. K. Attipoe, W. Zhang, and B. K. Datta, "A mathematical model to assess the impact of testing and isolation compliance on the transmission of COVID-19," *Infectious Disease Modelling*, vol. 8, no. 2, pp. 427–444, 2023.

[16] A. Malik, N. Kumar, and K. Alam, "Estimation of parameter of fractional order COVID-19 SIQR epidemic model," *Materials Today: Proceedings*, vol. 49, pp. 3265–3269, 2022.

[17] A. Malik, K. Alam, and N. Kumar, "Coefficient identification in SIQR model of inverse problem of COVID-19," *European Journal of Molecular and Clinical Medicine*, vol. 7, 2020.

[18] L. Wanika, J. R. Egan, N. Swaminathan, C. A. Duran-Villalobos, J. Branke, S. Goldrick, and M. Chappell, "Structural and practical identifiability analysis in bioengineering: a beginner's guide," *Journal of Biological Engineering*, vol. 18, no. 1, p. 20, 2024.

[19] U. Abdullah, Ş. Arslan, H. S. Manap, T. Gürkan, M. Çalışkan, A. Dayıoğlu, H. N. Efe, M. Yılmaz, A. Z. İbrahimoğlu, E. Gültekin, R. Durna, R. Başar, F. B. Osmanoğlu, and S. Ören, "Türkiye COVID-19 pandemi izleme ekranı," [Online]. Available: https://turcovid19.com/, August 2020.

[20] N. Tuncer, A. Timsina, M. Nuno, G. Chowell, and M. Martcheva, "Parameter identifiability and optimal control of an SARS-CoV-2 model early in the pandemic," *Journal of Biological Dynamics*, vol. 16, no. 1, pp. 412–438, 2022.

[21] A. Raue, C. Kreutz, T. Maiwald, J. Bachmann, M. Schilling, U. Klingmüller, and J. Timmer, "Structural and practical identifiability analysis of partially observed dynamical models by exploiting the profile likelihood," *Bioinformatics*, vol. 25, no. 15, pp. 1923–1929, 2009.

[22] J. K. Hale, "Functional differential equations," in *Analytic Theory of Differential Equations: The Proceedings of the Conference at Western Michigan University, Kalamazoo, from 30 April to 2 May 1970*. Berlin, Heidelberg: Springer Berlin Heidelberg, Aug. 2006, pp. 9–22.

[23] C. Kreutz, A. Raue, and J. Timmer, "Likelihood based observability analysis and confidence intervals for predictions of dynamic models," *BMC Systems Biology*, vol. 6, pp. 1–9, 2012.

[24] R. Dong, C. Goodbrake, H. Harrington, and P. G., "Differential elimination for dynamical models via projections with applications to structural identifiability," *SIAM Journal on Applied Algebra and Geometry*, vol. 7, no. 1, pp. 194–235, 2023.

[25] G. Chowell, S. Dahal, Y. R. Liyanage, A. Tariq, and N. Tuncer, "Structural identifiability analysis of epidemic models based on differential equations: a tutorial-based primer," *Journal of Mathematical Biology*, vol. 87, no. 6, p. 79, 2023.

[26] E. Walter and L. Pronzato, *Identifiability of Parametric Models: From Experimental Data*. Springer, 1997.

[27] U. Abdullah, Ş. Arslan, H. S. Manap, T. Gürkan, M. Çalışkan, A. Dayıoğlu, H. N. Efe, M. Yılmaz, A. Z. İbrahimoğlu, E. Gültekin, R. Durna, R. Başar, F. B. Osmanoğlu, and S. Ören, "Türkiye'de COVID-19 pandemisinin monitorizasyonu için interaktif ve gerçek zamanlı bir web uygulaması: TURCOVID19 (An interactive web-based dashboard for COVID-19 pandemic in real-time monitorization in Türkiye: TURCOVID19)," *Anadolu Kliniği Tıp Bilimleri Dergisi*, vol. 25, no. Special Issue on COVID-19, pp. 154–155, 2020.

[28] N. Tuncer and T. T. Le, "Structural and practical identifiability analysis of outbreak models," *Mathematical Biosciences*, vol. 299, pp. 1–18, 2018.

[29] H. Pohjanpalo, "System identifiability based on the power series expansion of the solution," *Mathematical Biosciences*, vol. 41, no. 1–2, pp. 21–33, 1978.

[30] G. Massonis and A. F. Villaverde, "Finding and breaking Lie symmetries: implications for structural identifiability and observability in biological modelling," *Symmetry*, vol. 12, no. 3, p. 469, 2020.

[31] Y. Lecourtier, F. Lamnabhi-Lagarrigue, and E. Walter, "Volterra and generating power series approaches to identifiability testing," *Identifiability of Parametric Models*, pp. 50–66, 1987.

[32] L. Ljung and T. Glad, "On global identifiability for arbitrary model parametrizations," *Automatica*, vol. 30, no. 2, pp. 265–276, 1994.

[33] J. Bezanson, A. Edelman, S. Karpinski, and V. B. Shah, "Julia: A fresh approach to numerical computing," *SIAM Review*, vol. 59, no. 1, pp. 65–98, 2017.

[34] R. Dong, C. Goodbrake, H. A. Harrington, and G. Pogudin, "Differential elimination for dynamical models via projections with applications to structural identifiability," *SIAM Journal on Applied Algebra and Geometry*, vol. 7, no. 1, pp. 194–235, 2023.

[35] Y. R. Liyanage, N. Heitzman-Breen, N. Tuncer, and S. M. Ciupe, "Identifiability investigation of within-host models of acute virus infection," 2024. [Online]. Available: https://www.biorxiv.org/content/early/2024/05/10/2024.05.09.593464

[36] F.-G. Wieland, A. L. Hauber, M. Rosenblatt, C. Tönsing, and J. Timmer, "On structural and practical identifiability," *Current Opinion in Systems Biology*, vol. 25, pp. 60–69, 2021.

[37] A. Raue, J. Karlsson, M. P. Saccomani, M. Jirstrand, and J. Timmer, "Comparison of approaches for parameter identifiability analysis of biological systems," *Bioinformatics*, vol. 30, no. 10, pp. 1440–1447, 2014.

[38] I. Siekmann, J. Sneyd, and E. J. Crampin, "MCMC can detect nonidentifiable models," *Biophysical Journal*, vol. 103, no. 11, pp. 2275–2286, 2012.

[39] L. E. Eberly and B. P. Carlin, "Identifiability and convergence issues for Markov chain Monte Carlo fitting of spatial models," *Statistics in Medicine*, vol. 19, no. 17–18, pp. 2279–2294, 2000.

[40] M. Joshi, A. Seidel-Morgenstern, and A. Kremling, "Exploiting the bootstrap method for quantifying parameter confidence intervals in dynamical systems," *Metabolic Engineering*, vol. 8, no. 5, pp. 447–455, 2006.

[41] J. A. Jacquez and P. Greif, "Numerical parameter identifiability and estimability: Integrating identifiability, estimability, and optimal sampling design," *Mathematical Biosciences*, vol. 77, no. 1–2, pp. 201–227, 1985.

[42] "Data2Dynamics software," 2024. [Online]. Available: https://github.com/Data2Dynamics

[43] A. Raue, B. Steiert, M. Schelker, C. Kreutz, T. Maiwald, H. Hass, J. Vanlier, C. Tönsing, L. Adlung, R. Engesser, et al., "Data2Dynamics: a modeling environment tailored to parameter estimation in dynamical systems," *Bioinformatics*, vol. 31, no. 21, pp. 3558–3560, 2015.

[44] A. Raue, M. Schilling, J. Bachmann, A. Matteson, M. Schelke, D. Kaschek, S. Hug, C. Kreutz, B. D. Harms, F. J. Theis, et al., "Lessons learned from quantitative dynamical modeling in systems biology," *PLOS ONE*, vol. 8, no. 9, p. e74335, 2013.

[45] G. Pogudin, "Speeding things up via linear first integrals," 2024. [Online]. Available: https://github.com/SciML/StructuralIdentifiability.jl/issues/63

[46] Soulaimani, A. Kaddar, and F. A. Rihan, "Stochastic stability and global dynamics of a mathematical model for drug use: Statistical sensitivity analysis via PRCC," *Partial Differential Equations in Applied Mathematics*, vol. 12, p. 100964, 2024.

[47] S. Marino, I. B. Hogue, C. J. Ray, and D. E. Kirschner, "A methodology for performing global uncertainty and sensitivity analysis in systems biology," *Journal of Theoretical Biology*, vol. 254, no. 1, pp. 178–196, 2008.

[48] K. Lab, "Our approach to uncertainty and sensitivity analysis (with R and MATLAB codes for use)," 2020. [Online]. Available: http://malthus.micro.med.umich.edu/lab/usanalysis.html

[49] S. Zhang, J. Ponce, Z. Zhang, G. Lin, and G. Karniadakis, "An integrated framework for building trustworthy data-driven epidemiological models: Application to the COVID-19 outbreak in New York City," *PLOS Computational Biology*, vol. 17, no. 9, p. e1009334, 2021.

[50] C. Elias, A. Sekri, P. Leblanc, M. Cucherat, and P. Vanhems, "The incubation period of COVID-19: A meta-analysis," *International Journal of Infectious Diseases*, vol. 104, pp. 708–710, 2021.

APPENDIX

We present the details of the transformation applied to model (1) to speed up the analysis in Julia, where the variable x1 t0 x9 represents the variables in model (1).

```
# Transformation #1
# Observe that: x1' + x2' + x9' +  y1 / rho = 0
# Therefore: x1 + x2 + x9 + int_y1 / rho = C1 for some constant C1
# We introduce new state int_y1' = 1/14 * rho * x2 and make it an output
# Then we can use x1 = C1 - x2 - x9 - int_y1 / rho to eliminate x1 from the system

# Transformation #2
# Observe that: x3' + x4' + x5' + x6' + x7' + x8' -  y1 / rho + y2 = 0
# Therefore: x3 + x4 + x5 + x6 + x7 + x8 - int_y1 / rho + int_y2 = C2 for some constant C2
# We introduce new state int_y2' = muh*x5 + muICU*x6 + muv*x7 and make it an output
# Then we can use x4 = C2 - x3 - x5 - x6 - x7 - x8 + int_y1 / rho - int_y2 to eliminate x4 from the system
```

The code for structural identifiability analysis is given below:

```
ode = @ODEmodel(
    x2'(t) = (betae*x2(t) + betan*x3(t) + betas*(C2 - (x3(t)+x5(t)+x6(t)+x7(t)+x8(t)) + int_y1(t) / rho - int_y2 ))*((C1 - x2(t) - x9(t) - int_y1(t) / rho)/((C1 - x2(t) - x9(t) - int_y1(t) / rho)+x2(t)+x3(t)+(C2 - (x3(t)+x5(t)+x6(t)+x7(t)+x8(t)) + int_y1(t) / rho - int_y2 )+x8(t)+x9(t))) - (1/14)*x2(t),
    x3'(t) = (1-rho)*(1/14)*x2(t) - (gamman)*x3(t),
```

```
x5'(t) = alpha1*(C2 - (x3(t)+x5(t)+x6(t)+x7(t)+x8(t)) + int_y1(t) / rho - int_y2 ) - (alpha2+gammah + muh)*x5(t),

x6'(t) = alpha2*x5(t) - (alpha3+gammaICU+muICU)*x6(t),

x7'(t) = alpha3*x6(t) - (gammav + muv)*x7(t),

x8'(t) = gamman*x3(t) + gammas*(C2 - (x3(t)+x5(t)+x6(t)+x7(t)+x8(t)) + int_y1(t) / rho - int_y2 ) + gammah*x5(t) + gammaICU*x6(t) + gammav*x7(t),

x9'(t) = eta*(C1 - x2(t) - x9(t) - int_y1(t) / rho),

int_y1'(t) = (1/14) * rho * x2(t),

int_y2'(t) = muh*x5(t) + muICU*x6(t) + muv*x7(t),

y1(t) = (1/14)*rho*x2(t),

y2(t) = muh*x5(t) + muICU*x6(t) + muv*x7(t),

y3(t) = x6(t),

y4(t) = x7(t),

y5(t) = int_y1(t),

y6(t) = int_y2(t),

)


println(assess_identifiability(ode, known_ic=[x2,x3,x5,x6,x7,x8,x9]))
```